



# AMERICAN METEOROLOGICAL SOCIETY

*Monthly Weather Review*

## EARLY ONLINE RELEASE

This is a preliminary PDF of the author-produced manuscript that has been peer-reviewed and accepted for publication. Since it is being posted so soon after acceptance, it has not yet been copyedited, formatted, or processed by AMS Publications. This preliminary version of the manuscript may be downloaded, distributed, and cited, but please be aware that there will be visual differences and possibly some content differences between this version and the final published version.

The DOI for this manuscript is doi: 10.1175/MWR-D-18-0308.1

The final published version of this manuscript will replace the preliminary version at the above DOI once it is available.

If you would like to cite this EOR in a separate work, please use the following full citation:

Chantry, M., T. Thorne, T. Palmer, and P. Düben, 2018: Scale-selective precision for weather and climate forecasting. *Mon. Wea. Rev.* doi:10.1175/MWR-D-18-0308.1, in press.

© 2018 American Meteorological Society



# Scale-selective precision for weather and climate forecasting

Matthew Chantry\*, Tobias Thorne, Tim Palmer

*Atmospheric, Oceanic and Planetary Physics, University of Oxford, UK*

Peter Düben

*European Centre for Medium-Range Weather Forecasts, Reading, UK*

1

2

3

4

5

6

7

8

\*Corresponding author address: Atmospheric, Oceanic and Planetary Physics, University of Oxford, UK

E-mail: matthew.chantry@physics.ox.ac.uk

## ABSTRACT

Attempts to include the vast range of lengthscales and physical processes at play in the Earth's atmosphere push weather and climate forecasters to build and more efficiently utilise some of the most powerful computers in the world. One possible avenue for increased efficiency is in using less precise numerical representations of numbers. If computing resources saved can be reinvested in other ways (e.g. increased resolution or ensemble size) a reduction in precision can lead to an increase in forecast accuracy. Here we examine reduced numerical precision in the context of ECMWF's OpenIFS model. We posit that less numerical precision is required when solving the dynamical equations for shorter lengthscales while retaining accuracy of the simulation. Transformations into spectral space, as found in spectral models such as OpenIFS, enact a lengthscale decomposition of the prognostic fields. Utilising this, we introduce a reduced precision emulator into the spectral space calculations and optimise the precision necessary to achieve forecasts comparable with double- and single-precision. On weather forecasting timescales, larger lengthscales require higher numerical precision than smaller lengthscales. On decadal timescales, half-precision is still sufficient precision for everything except the global mean quantities.

27 **1. Introduction**

28 Improving the efficiency of weather and climate forecasts is essential in a world struggling to  
29 predict and adapt to anthropogenic climatic change and its associated weather extremes. More  
30 accurate forecasts will require numerical models of Earth’s atmosphere to become more com-  
31 prehensive in the processes they capture, to operate at higher resolutions and to employ larger  
32 ensembles during simulations. All of this comes at an increased computational cost, however, and  
33 there is a limit to the computational cost of forecasts that forecasting centres can afford. While the  
34 peak performance of supercomputers continues to increase, individual processors have ceased to  
35 get faster in recent years, so that more processors must be run in parallel. However, an increase  
36 in the number of processors incurs a proportional energy cost that may become unaffordable in  
37 the near future. Using computer resources more efficiently is therefore a requirement to achieve  
38 a substantial increase in forecast accuracy. Typically simulations run at less than 5% of peak  
39 supercomputer performance as data movement, both within and between cores, dominates the  
40 computational burden.

41 Conventionally, most numerical models use double-precision floating-point values to represent  
42 real numbers during calculations, assigning 64 bits of precision to each number. However, there  
43 is no a priori reason why 64 bits should be the optimal number to use. Reducing the number of  
44 bits to less than the double-precision default poses the risk of increased rounding errors or even  
45 the inability to represent the number. For instance, single-precision (32 bits total) has a maximum  
46 relative error of  $2^{-23}$  and can represent numbers up to approximately  $3.4 \times 10^{38}$ , whereas half-  
47 precision (16 bits total) represents numbers up to 65504 with a maximum relative error of  $2^{-10}$   
48 (IEEE 2008). There is no IEEE standard for lower precision than this, for which applications have  
49 been historically few.

50 No model of the weather or climate yields perfect forecasts, regardless of the precision used, as a  
51 result of observational and modelling errors. For example, the observations used to generate initial  
52 conditions for forecasts are of an inevitably limited accuracy and spatial density, and are certainly  
53 not accurate to many decimal places that would justify a representation in double-precision. Data  
54 assimilation routines are imperfect when feeding observations into the model simulation, and any  
55 numerical method to solve the non-linear equations that describe the fundamental physics of the  
56 atmosphere in the model itself will always introduce further errors. Primarily, such errors arise  
57 from the model's finite resolution, which means that there are always sub-grid-scale phenomena  
58 that cannot be explicitly resolved and whose effects must instead be approximated through param-  
59 eterisation.

60 A number of recent studies have shown that accurate forecasts could be produced at a much  
61 lower computational cost by running parts of both full-complexity and more idealised weather  
62 and climate models in reduced precision. Düben and Palmer (2014) first demonstrated that the  
63 OpenIFS could be run entirely in single-precision (32 bits) producing reasonable results, and Váňa  
64 et al. (2017) demonstrated for IFS that model quality in single-precision was very comparable  
65 to double-precision simulations while a forty per cent reduction of run-time could be achieved.  
66 Nakano et al. (2018) showed small errors and a 46% reduction in runtime when running the Non-  
67 hydrostatic Icosahedral Grid Atmospheric Model (NICAM) with the majority of calculations at  
68 single-precision. Even lower precision has been successfully applied to the Intermediate Global  
69 Climate Model (IGCM), for which Düben and Palmer (2014) estimate that 98% of the model  
70 could be run with 20 bits to represent real numbers (8 bit significand) to yield better forecasts than  
71 a double-precision but lower-resolution alternative with similar computational costs.

72 In the absence of real reduced-precision hardware capable of running full-complexity models  
73 in less than single-precision the effects of reduced precision can be emulated on double-precision

hardware (see section 3). However, there is tangible evidence for the potential benefit of reduced precision computing. Russell et al. (2015) used Field Programmable Gate Arrays (FPGAs), which are difficult to program but can apply user-specified precision, to run the idealised Lorenz ‘96 model atmosphere in less than half-precision (16 bits) and demonstrated considerable speed-ups relative to double-precision with negligible loss of accuracy. With the advent of the “Volta” Graphical Processing Unit (GPU) and Tensor Core produced by NVIDIA half-precision hardware will become available to forecast centres (provided that forecast models are able to run on GPUs). Volta can run in double-, single- or half-precision with a linear decrease in power requirements per calculation as the precision is reduced (NVIDIA 2018). The Tensor Core on NVIDIA Volta GPUs is 16 times faster when multiplying half-precision matrices when compared with double-precision. There is a strong demand for ‘mixed precision’ architectures in ‘deep learning’ artificial intelligence applications. This paper is part of a body of work investigating whether weather and climate forecasters could benefit from this trend.

The Earth System shows non-linear and chaotic behavior. It is difficult to identify the optimal level of precision in such a system. However, to guide a reduction in precision it has been suggested to reduce numerical precision for computations of small spatial scales while keeping precision high for computations that calculate large-scale behaviour (Düben and Palmer 2014; Thornes et al. 2018). Small scale dynamics are inherently uncertain due to the strong influence of parametrisation schemes at these scales as well as fast error growth and limited skill in the assimilation of atmospheric observations. The approach to reduce precision with spatial scale has already been demonstrated to yield accurate forecasts in models of low and medium complexity, namely Lorenz’96 and the Surface Quasi-Geostrophic (SQG) equations (Thornes et al. 2017, 2018). It was shown that the smallest scales (highest wavenumbers) of a simulation in SQG could be represented with just 5 bits in the significand with negligible impact on the accuracy. Results in Düben

<sup>98</sup> and Palmer (2014) suggests that the same approach can also be realised in a three-dimensional  
<sup>99</sup> spectral dynamical core.

<sup>100</sup> This paper will describe a series of experiments designed to test whether precision can be re-  
<sup>101</sup> duced beyond single precision without impairing the forecast accuracy in the Open Integrated  
<sup>102</sup> Forecasting System (OpenIFS) developed by the European Centre for Medium-Range Weather  
<sup>103</sup> Forecasts (ECMWF). OpenIFS is the portable version of ECMWF's operational weather forecast  
<sup>104</sup> model IFS. This study emulates low precision in the ECMWF OpenIFS and applies, for the first  
<sup>105</sup> time, a scale-selective approach to this system. Precision is reduced more at the less certain small  
<sup>106</sup> spatial scales within the spectral part of the model, where variables are represented through dif-  
<sup>107</sup> ferent wavenumber components corresponding to different spatial scales and scale-selectivity is  
<sup>108</sup> hence possible.

<sup>109</sup> The rest of this paper is organised as follows. Section 2 outlines the OpenIFS in more detail,  
<sup>110</sup> whilst section 3 describes the implementation of emulated reduced precision therein. Section 4  
<sup>111</sup> describes a number of experiments designed to test the proficiency of scale-selective precision in  
<sup>112</sup> OpenIFS and presents the results. The findings are discussed in section 5, and the paper concludes  
<sup>113</sup> with a discussion of the potential implications.

## <sup>114</sup> 2. OpenIFS

<sup>115</sup> The European Centre for Medium-Range Weather Forecasts produces global forecasts using the  
<sup>116</sup> Integrated Forecast System (IFS). At the time of writing, the latest operational model is version  
<sup>117</sup> 43r3, released in July 2017, which produces a single ten-day global forecast at 9 km horizontal  
<sup>118</sup> resolution with 137 vertical levels and a fifteen-day fifty-member ensemble global forecast at 18  
<sup>119</sup> km horizontal resolution with 91 vertical levels (ECMWF 2017a).

120 For research activities external to ECMWF the centre makes available a portable version of the  
121 model, called “OpenIFS”, which is available for licensed researchers to download and use re-  
122 mately. The OpenIFS has all the forecast functionality of the operational IFS including all the  
123 parameterisation schemes, and contains some half a million lines of code distributed across more  
124 than two thousand files. The version of OpenIFS that is employed here is based on the ‘38r1’  
125 release of IFS, which was used operationally until June 2013, in a fully-functional format except  
126 for the data assimilation and ensemble-forecasting components. In this study the maximum res-  
127 olution at which OpenIFS is run is ‘TL511’, which corresponds to 512 wavenumber components  
128 (from 0 to 511) in spectral space and a triangular-linear reduced-Gaussian grid of approximately  
129 40 km horizontal resolution. By contrast, from January 2010 to March 2016 (a timespan covering  
130 most of the test-cases presented here) the ECMWF’s operational releases of IFS used a “TL639”  
131 resolution for its ensemble, which corresponds to 640 wavenumber components and roughly 32km  
132 horizontal resolution.

133 The OpenIFS uses a semi-Lagrangian, semi-implicit numerical scheme to solve the Navier–  
134 Stokes equations for the momentum, surface pressure, temperature, geopotential and vertical ve-  
135 locity of atmospheric fluid parcels at each timestep. For the implicit part of the timestepping fields  
136 are transformed to spectral space through Fourier and Legendre transforms.

### 137 **3. Reduced precision emulation in OpenIFS**

Conventionally, most numerical models use double-precision floating-point values to represent  
all variables during calculations, assigning 64 bits of precision to each number. Of these, 1 bit  
represents the sign of the number (+1 or -1),  $E$  bits represent the exponent (the highest power  
of two that the number is greater than) and  $S$  bits represent the significand (the number’s exact  
multiple, somewhere between 1 and 2, of this power) according to standards set by the IEEE

(2008). The overall number is given by,

$$N = \pm S \times 2^E,$$

where the value of each bit in the significand,  $b_i$ , or the exponent,  $c_j$ , is either 0 or 1, the significand and exponent are given by,

$$S = 1 + \sum_{i=0}^{51} b_i 2^{-i}, \quad E = \sum_{j=0}^{10} c_j 2^j - 1023.$$

<sup>138</sup> This means that the significand is a fraction between 1 and 2. All “normal” numbers representable  
<sup>139</sup> in double-precision lie between  $2^{-1022}$  and  $2^{1023}$ , with minimum a spacing of  $2^{-41}$ . Any number  
<sup>140</sup> outside this spacing will be rounded to the nearest resolvable value; numbers outside the resolvable  
<sup>141</sup> range will be rounded to zero or infinity.

<sup>142</sup> To emulate the effects of reduced precision hardware that does not strictly follow the IEEE stan-  
<sup>143</sup> dard requires a special ‘emulator’ program to be compiled and run alongside the standard modules  
<sup>144</sup> included within the OpenIFS (Dawson and Düben 2016). Alterations to the main program that are  
<sup>145</sup> required are minimal. The modified program induces reduced precision by treating variables as  
<sup>146</sup> Fortran derived types that are defined by the emulator. Each variable of this type contains a value  
<sup>147</sup> and a precision (number of significand bits). For each operation involving these derived types  
<sup>148</sup> the values are passed in, operated on, and then truncated to the specified number of bits. In this  
<sup>149</sup> way, the main program always runs using double-precision floating point numbers and double-  
<sup>150</sup> precision hardware throughout, but its output is the same as that would be obtained using mixed  
<sup>151</sup> precision hardware. The extra costs associated with emulated precision result in computations that  
<sup>152</sup> are slower than standard double-precision arithmetic. Real mixed precision hardware would not  
<sup>153</sup> go through this process of rounding numbers and would therefore entail no such costs. Hence, the  
<sup>154</sup> emulator cannot be used to analyse the potential computational cost savings that such hardware  
<sup>155</sup> would yield, only the effect that it might have on the accuracy of the model being run. In this

156 study we investigate the impact of the number of bits used in the significand, which controls the  
157 precision of a floating-point number. The IEEE standard representations of double-, single- and  
158 half-precision use 52, 23 and 10 bits respectively to represent the significand.

159 The size of OpenIFS’s code-base make the complete introduction of the emulator a challenging  
160 undertaking. When combined with the increased computation overhead for running the emulator,  
161 we decide to introduce the emulator in only a portion of the code-base. Building upon the scale-  
162 selective work of Thorne et al. (2018) we select those computations carried out in spectral space.

163 Although this area has a relatively small computational cost, there are interesting scientific ques-  
164 tions to be asked for the information content required for these modes. The largest uncertainties  
165 and shortest predictable timescales are for short lengthscales. In spectral space, fields are decom-  
166 posed by lengthscale and phase, represented by complex spectral coefficients. Linear calculations  
167 on these coefficients are then carried out, with no interaction between coefficients representing suf-  
168 ficiently different lengthscales (derivatives of fields involve interactions between adjacent modes).  
169 This enables the use of different precision levels for calculations at different lengthscales, which  
170 we shall here investigate.

171 In the timestepping loop, the explicit terms in the dynamics equations are transformed from grid-  
172 point to spectral space. Horizontal wind components are converted to a vorticity and divergence  
173 representation. Beyond this point reduced precision is used for all calculations up to the point  
174 where vorticity and divergence fields are converted back to wind components. This choice for re-  
175 duced precision introduction was motivated by the code structure. Here, global precision reduction  
176 will refer to a fixed precision level being used for all spectral space calculations. Scale-selective  
177 precision will involve precision dependent upon the total wavenumber,  $n$ . This is achieved by  
178 element-wise changes to the number of significant bits used for all vectors and arrays containing  
179 spectral coefficients.

180 While vector and array calculations dominate, there are also calculations involving scalar fields  
181 and literals which take their precision from a global significant bits variable. This number has a  
182 limited impact on the accuracy of our forecasts, but is typically set to match the highest precision  
183 used in array and vector calculations. This choice, made to limit the changes to the code base,  
184 could permit precision to leak in individual calculations. However the outputs of these calculations  
185 are stored in vectors or arrays with scale-selective prescribed precision where the correct precision  
186 will be restored. On real hardware the slowdown introduced by occasional use of double-precision  
187 scalar variables will not be significant as floating-point operations (flops) are typically not the  
188 computational bottleneck.

## 189 **4. Results**

### 190 *a. Test case: Hurricane Sandy*

191 We begin with a hindcast of hurricane Sandy, to test the impact of global precision reduction.  
192 In figure 1 we plot the hurricane path from the forecast start-date, 2012/10/27, until landfall on  
193 2012/10/29. A resolution of T255 (80km horizontal grid), with 91 vertical levels is used, with a  
194 time step of 45 minutes. Although the hurricane centre varies slightly between precision levels,  
195 the strength (not plotted), landfall location and landfall time are constant for precision levels down  
196 to 8 significand bits.

197 In contrast, the geopotential height of pressure level 500hPa (Z500) is significantly changed by  
198 this lowest precision (figure 2). After 5 days, there is a clear global bias in Z500. This can be  
199 ascribed to representing large mean quantities, such as geopotential or temperature with few sig-  
200 nificant bits. The global mean for the double-precision Z500 is 5648.47m, compared to the 8-bit  
201 significand value of 5690.89m. Representing values of this magnitude with 8-bit significands can

202 only be achieved to the nearest 16m, an unacceptable level of accuracy. This issue of large global  
 203 means also affects the temperature field. Values with magnitude 300 have a spacing (between  
 204 neighbouring representable numbers) of approximately 1 degree. Here, the use of Kelvin instead  
 205 of Celsius may be considered a waste of bits. Rewrite 300K as 26.8125°C and the spacing is  
 206 decreased below 0.1°C. Renormalising the variables, in the right context, change the viability of  
 207 using half-precision in general circulation models. In spectral space, there is a clear route forward:  
 208 the precision used should be dependent on the total wavenumber. The zeroth mode of a spherical  
 209 harmonic expansion represents the global mean of the field, where the unit choice of fields is the  
 210 most significant. In figure 2(d), we plot Z500 for a forecast with double-precision used for cal-  
 211 culations in spectral space involving the zeroth spectral mode, and 8 significand bits for all other  
 212 modes. This produces a global mean Z500 of 5649.54m, to be compared with double, 5648.47m  
 213 and single, 5648.79m.

#### 214 *b. Error measures*

215 The hurricane Sandy forecast demonstrates the value of scale-selectively setting the precision as  
 216 a function of wavenumber, but lacks rigour when it comes to finding the optimal precision. To this  
 217 end we introduce two measures which we will use to assess reduced precision experiments.

The first error measure uses the distance between double-precision and single-precision (for  
 spectral space) forecasts. Váňa et al. (2017) noted noticeable reduction in accuracy when running  
 IFS with a majority of calculations in single-precision. We define the horizontal  $L_2$ -norm over  
 model levels as

$$L_2^2(f) = \int_{\theta=0}^{2\pi} \int_{\lambda=0}^{\pi} f(\lambda, \theta, z)^2 \sin \lambda \, d\lambda \, d\theta.$$

We define  $Er$  as the supremum of the ratio of horizontal  $L_2$ -norm errors between a field integrated  
 forward at reduced precision,  $f_r$  relative to the distance between double,  $f_d$  and single-precision,

$f_s$ , integrations,

$$Er(f) = \sup_z \left( \frac{L_2^2(f_r(\lambda, \theta, z) - f_d(\lambda, \theta, z))}{L_2^2(f_s(\lambda, \theta, z) - f_d(\lambda, \theta, z))} \right),$$

218 where  $nlev$  are the model levels. We consider  $Er$  for prognostic variables surface pressure, temper-  
219 ature, vorticity and divergence at day two. A reduced precision forecast is considered acceptable if  
220  $Er$  is less than 2 for all 4 fields. Calculating this measure after longer integration times consistently  
221 gave weaker precision constraints.

222 The second error measure used here attempts to use information from the ECMWF ensemble  
223 standard deviation to capture the uncertainty in the model. Considering Z500 over Europe, we  
224 calculate the proportion of grid-points that lie more than one standard deviation away from a  
225 double-precision forecast. The European region is used because the test-cases were chosen on  
226 the basis of selecting a wide variety of atmospheric conditions in the European region. Assuming  
227 normality, we consider a forecast acceptable if less than a third of grid-points lie more than one  
228 standard deviation of the operational forecast ensemble from the double-precision forecast. This  
229 is measured over days 2 to 5 of the forecast. Day 1 is excluded as the ensemble standard deviation  
230 is very small during day 1, so an accurate 5 day forecast appears inaccurate if precision is adjusted  
231 to day 1.

232 For the study below, we use resolutions significantly below operational values which prevents the  
233 fair comparison of reduced precision models using observations. Our aim with the two measures  
234 introduced is to provide approximate upper and lower bounds on acceptable precision. The  $L_2$ -  
235 norm sets a very tight error threshold, aiming to provide a model very close to double-precision.  
236 In contrast, the ensemble-spread measure attempts to create a model within the uncertainty of an  
237 ECMWF probabilistic forecast. Given that the probabilistic forecast incorporates initial condition  
238 uncertainty and stochastic physics (ECMWF (2017)), neither of which are part of our reduced

239 precision models, this creates a weaker error constraint. Together these two should provide a  
240 guide for an optimal precision setup.

241 We consider four start dates for the following study, 2009/10/26 00:00, 2010/02/11 00:00,  
242 2013/10/26 00:00 and 2014/02/11 00:00. These dates cover two recent UK storm conditions in  
243 2013 and 2014, as well as the same calendar date four years earlier which exhibited calm condi-  
244 tions for the UK.

245 *c. Optimal precision*

In figure 3(a) we plot the necessary precision for total wavenumbers greater than or equal to  $n$  to satisfy the  $L_2$ -norm measure for four T255 integrations (crosses) and the average. There is little start-date dependence and a trend towards lower precision being required at higher wavenumbers. A similar pattern is found when reducing precision only for a single total wavenumber (not plotted). Figure 3(b) plots the average precision against wavenumber for both norms at two resolutions: T159 and T255. The ensemble error gives a lower precision requirement, particularly for small wavenumbers. For both datasets, noticeably higher precision is required for the first five wavenumbers. As the truncation limit is reached, the necessary precision rapidly decreases to levels equivalent to one significant figure. This is illustrated in figure 3(c) where the T255 data is transformed to lengthscale and relative error using the formulae

$$\text{Relative error} = 2^{-\text{Significand bits}}, \quad \text{Lengthscale} = \frac{C_{\text{Earth}}}{2n}.$$

246 After rescaling the data by  $N$ , the truncation limit, we see good agreement between the two dif-  
247 ferent resolutions (figure 3d). This suggests a trend whereby necessary precision is a function of  
248 normalized total wavenumber,  $n/N$ . Extrapolating to operational resolutions, this scaling would  
249 predict a delay in total wavenumber from which low precision could be used. This will required

250 a high resolution study to investigate. The number of bits used to store the state vector could be  
251 significantly decreased if only the bits used for integration were stored. Even when maintaining  
252 a double-precision length exponent (11 bits), the number of bits used to store the T255 spectral  
253 space vector is decreased by over 70%. The observed scaling of precision as a function of  $n/N$   
254 results in savings that are independent of the resolution.

255 *d. Decadal runs*

256 The motivations for reduced numerical precision for weather forecasts are equally valid for  
257 climate predictions. Here we wish to test the impacts of reduced numerical precision on long time  
258 integration. For this we run the following experiment: initial conditions from 1st-10th of January  
259 2005 are integrated forward to the end of 2015 with prescribed observed SSTs. Discarding the data  
260 from 2005 we have a ten member ensemble for the decade 2006-2015. The model resolution is  
261 T159 with 91 levels and is forced with identical sea-surface temperatures for all runs. We consider  
262 three different numerical precisions: single, scale-selective and half-precision. Each is compared  
263 with a double-precision ‘truth’ ensemble. Scale-selective precision is based-upon the results from  
264 weather prediction. Specifically, scale-selective means double-precision for the zero mode, 11  
265 significant bits for total wavenumbers 1 to 50, 9 significand bits for the next 50 and 7 significand  
266 bits for the higher modes (see dashed grey lines in figure 3c). This is generally a cautious approach  
267 compared to our results, with the chosen precision being larger than that required for weather  
268 predictions with the exception of the first six (non-zero) modes. The importance of precision to  
269 these modes was found to decay with lead time, with 11 bits being acceptable beyond day 5. Half-  
270 precision uses the 10 bit significand for all non-zero modes, with the zeroth mode calculated in  
271 double-precision (indicated by “zm”). The exponent for all precision levels is kept at the double-  
272 precision value of 11 bits. For each precision we calculate the paired t-test, testing for significantly

273 different decadal averages of precipitation, 2m temperature and surface pressure from the double-  
274 precision 10 member ensemble. In figure 4, we plot maps of the probability implied by the t-test  
275 at the 1%, 5% and 10% levels. To test the significance of each field at each precision we use the  
276 False Discovery Rate (FDR) test (Benjamini and Hochberg 1995; Wilks 2006). This test examines  
277 the distribution of grid-point  $p$ -values, ordered by their magnitude, to find those that lie below the  
278 line described by  $\text{FDR}(n) = \frac{n}{N}p$ , where  $n$  is the ordering index,  $N$  the total number of tests (here  
279 the number of grid-points) and  $p$  the global  $p$ -value for the test (here 5%). The distribution of  
280  $p$ -values for each field is shown in the top row of figure 5. For single-precision and half-precision  
281 (zm) all points lie above the FDR line and so no fields are found to be significantly different.  
282 For the scale-selective precision the mean surface pressure is found to significantly differ from  
283 double-precision. All grid-points with  $p$ -values less than or equal to the largest failed p-value are  
284 classified as significantly different and are denoted by red dots in figure 4.

285 The bottom row of figure 5 shows the FDR test applied to ensembles at varying precision  
286 with the Stochastically Perturbed Parametrization Tendency (SPPT) scheme active. This scheme,  
287 used in the ECMWF ensemble, applies multiplicative noise, with prescribed correlations in space  
288 and time, to the accumulated tendencies of the parameterisation schemes (Buizza et al. 1999).  
289 The standard operational values for correlation lengthscales and timescales are used here (Shutts  
290 et al. 2011). This scheme has been shown to have a positive effect on both weather and climate  
291 timescales with not only increased ensemble spread but also changes in the mean state (Palmer  
292 et al. 2009; Weisheimer et al. 2014; Sanchez et al. 2016; Christensen et al. 2017). Examining each  
293 precision setup against a double-precision ensemble (also with SPPT active) we find that none of  
294 the measured fields are significantly different.

295 Establishing the optimal precision for climatological timescales will require more research. The  
296 results found here suggest that precisions far below single-precision are feasible for integrations

297 on long timescales. Measured against the spread of ensembles with SPPT the differences induced  
298 by precision reductions are small.

299 *e. Higher resolution weather forecasts*

300 The low computational cost of running at T159 and T255 enabled a thorough search of optimal  
301 precision and a guide for the necessary precision at operational resolutions. To test the effectiveness  
302 of this guide we now consider higher resolution forecasts at reduced precision. We consider  
303 9 start dates between 2011 and 2017 at a resolution of TL511 with 91 levels using a timestep of  
304 15 minutes. These start dates cover a range of months and conditions. The start dates considered  
305 are 2011/04/08 00:00, 2012/10/27 00:00, 2013/02/01 00:00, 2014/03/15 00:00, 2015/10/02 12:00,  
306 2016/03/07 00:00, 2016/06/30 00:00, 2017/08/25 00:00, 2017/09/05 12:00. The effective grid res-  
307 olution of approximately 39km is closer to ECMWF's 20km resolution (recently upgraded from  
308 31km in 2016). Using the same  $L_2$ -norm as before we plot the average error across start dates for  
309 temperature and surface pressure using scale-constant precision (figure 6(a-b)). Double-precision  
310 is used for the zeroth mode. Equivalent plots for vorticity and divergence are comparable and are  
311 not shown here. As significand bits is decreased, the error remains comparable to single-precision  
312 (close to 1) until 12 significant bits, below this the error increases rapidly. For surface pressure we  
313 see a small increase in error for 12 significand bits at 1 and 2 days which has no obvious impact  
314 on the 5 and 10 day values. Motivated by the fact that already available hardware supports 10 sig-  
315 nificant bits (half-precision) we next ask from which total wavenumber can we use 10 significand  
316 bits. In figure 6(c-d) we plot the temperature and surface pressure errors for simulations which  
317 use 12 significand for wavenumbers between 1 and  $n - 1$  and 10 significand bits for  $n$  and greater.  
318 Beyond  $n = 15$  we see no further impact of using 10 bits on our results (relative to using 12 bits  
319 globally). Considering only the error at days 5 and 10 this can be decreased to the 5th wavenum-

320 ber. A model with 10 significand bits from wavenumber 5 onwards treats over 99.98% of spectral  
321 coefficients with half-precision significands.

322 Finally we assess the high resolution simulations in the context of the ECMWF operational  
323 ensemble. For each start date and precision level we use the operational ensemble mean and  
324 ensemble standard deviation and calculate the proportion of the globe that lies more than one stan-  
325 dard deviation away from the mean. In figure 7 this measure is plotted against time for Z500 and  
326 850hP meridional winds for a selection of precision experiments. Here scale-selective is defined as  
327 12 significand bits for wavenumbers less than 5 and 10 significand bits for higher wavenumbers.  
328 Model version and resolution differences account for differences between the ECMWF control  
329 (green) and our double-precision simulations (dotted blue), which otherwise use the same unper-  
330 turbed initial condition. Relative to this difference, any precisions with more than 9 significand  
331 bits have equivalent performance. Perturbed members of the ECMWF ensemble lie close to the  
332 value of one-third. This would be expected for randomly drawn data from a normal distribution  
333 with the ensemble mean and ensemble standard deviation. These results are highly promising for  
334 doing operational forecasting at reduced precision. Relative to model changes and initial condition  
335 uncertainty reduced precision calculations have a small effect on this set of calculations.

## 336 5. Conclusion

337 We have presented here the effects of reduced precision in spectral space on the accuracy of  
338 ECMWF's OpenIFS system. This marks the latest step in the assessment of reduced precision for  
339 a hierarchy of weather and climate models. The necessary precision for an accurate weather model  
340 has clear scale-dependence, with large spatial scales requiring higher precision than small scales.  
341 Even at large scales the necessary precision is far below that of double-precision.

342 Towards operational resolutions we continue to find that double-precision is unnecessary, partic-  
343 ularly when examined in the context of the operational ensemble. When compared to the ECMWF  
344 ensemble spread, precision errors are small, but future work will need to study the spread of an  
345 ensemble when integrated at reduced-precision.

346 For decadal runs, the necessary precision again appears to be much lower than the double-  
347 precision widely used. Computational constraints have prevented a full search for optimal pre-  
348 cision over this timescale. However both of the reduced precision setups considered here are not  
349 significantly different from double-precision when SPPT is used for the ensembles. The resolution  
350 dependence of precision on weather timescales appears to be approximately linear in truncation  
351 level, with low precision simply delayed to higher wavenumbers as resolution is increased. The  
352 success of half-precision (with the zonal mode kept at double-precision) on decadal timescales  
353 implies that resolution increases will have a limited impact on the necessary precision for these  
354 timescales.

355 While the reduction of precision is still limited to a fairly small fraction of the computations of  
356 the full model, we will continue to investigate a precision reduction in more model components.  
357 This work can act as a first guide for the precision necessary for other calculations involved in a  
358 general circulation model. For example the Legendre transforms exhibit expensive scaling proper-  
359 ties as resolution is increased, due to the matrix-multiplications involved. Our work here suggests  
360 that half-precision is plausible for these calculations. Investigating the spectral transforms will be  
361 carried out in future work. The inherent uncertainty in physical parameterisation schemes make  
362 these schemes a natural place for further reduced precision studies.

363 **6. Acknowledgements**

364 M. Chantry was supported by a grant from the Office of Naval Research Global. P. D. Düben  
365 gratefully acknowledges funding from the Royal Society for his University Research Fellowship as  
366 well as funding from the ESIWACE project. ESIWACE has received funding from the European  
367 Union’s Horizon 2020 research and innovation programme under grant agreement No 675191.  
368 T. N. Palmer received funding from the European Research Council (ERC) under the European  
369 Union’s Horizon 2020 research and innovation programme (grant agreement no 741112). Ac-  
370 knowledgegement is made for the use of ECMWF’s computing and archive facilities in this research.

371 **References**

- 372 Benjamini, Y., and Y. Hochberg, 1995: Controlling the false discovery rate: a practical and power-  
373 ful approach to multiple testing. *Journal of the royal statistical society. Series B (Methodologi-*  
374 *cal)*, 289–300.
- 375 Buizza, R., M. Milleer, and T. Palmer, 1999: Stochastic representation of model uncertainties in  
376 the ecmwf ensemble prediction system. *Quarterly Journal of the Royal Meteorological Society*,  
377 **125 (560)**, 2887–2908.
- 378 Christensen, H., J. Berner, D. R. Coleman, and T. Palmer, 2017: Stochastic parameterization and  
379 el niño–southern oscillation. *Journal of Climate*, **30 (1)**, 17–38.
- 380 Dawson, A., and P. D. Düben, 2016: rpe v5: An emulator for reduced floating-point precision in  
381 large numerical simulations. *Geosci. Model Dev. Discuss., in review, doi, 10.*
- 382 Düben, P. D., and T. N. Palmer, 2014: Benchmark tests for numerical weather forecasts on inexact  
383 hardware. *Monthly Weather Review*, **142 (10)**, 3809–3829.

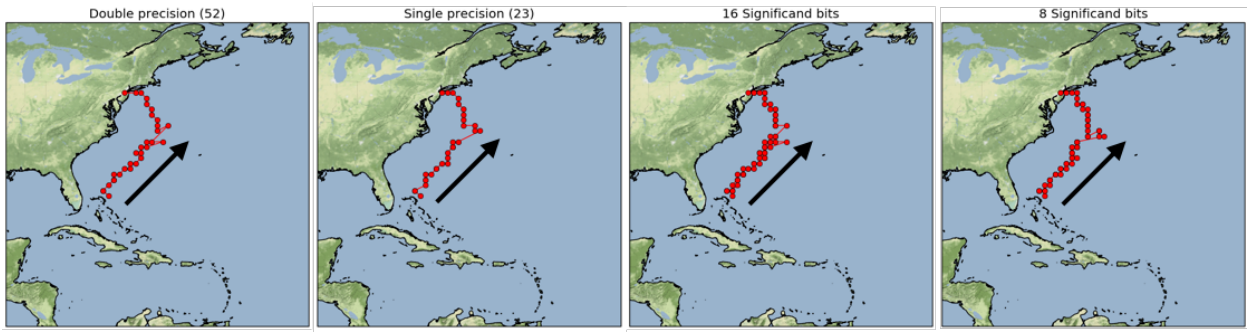
- 384 ECMWF, 2017: Ifs documentation cy43r3: Part V: Ensemble prediction system. Tech. rep.,
- 385 ECMWF: Shinfield Park, UK. URL <https://www.ecmwf.int/sites/default/files/elibrary/2017/17737-part-v-ensemble-prediction-system.pdf>.
- 386
- 387 Nakano, M., H. Yashiro, C. Kodama, and H. Tomita, 2018: Single precision in the dynamical
- 388 core of a nonhydrostatic global atmospheric model: Evaluation using a baroclinic wave test
- 389 case. *Monthly Weather Review*, **146** (2), 409–416, doi:10.1175/MWR-D-17-0257.1, URL <https://doi.org/10.1175/MWR-D-17-0257.1>, <https://doi.org/10.1175/MWR-D-17-0257.1>.
- 390
- 391 Palmer, T., R. Buizza, F. Doblas-Reyes, T. Jung, M. Leutbecher, G. Shutts, M. Steinheimer, and
- 392 A. Weisheimer, 2009: Stochastic parametrization and model uncertainty. *ECMWF Technical*
- 393 *Memoranda*, **598**, 1–42.
- 394
- 395 Russell, F. P., P. D. Düben, X. Niu, W. Luk, and T. N. Palmer, 2015: Architectures and preci-
- 396 sion analysis for modelling atmospheric variables with chaotic behaviour. *Field-Programmable*
- 397 *Custom Computing Machines (FCCM), 2015 IEEE 23rd Annual International Symposium on*,
- 398 IEEE, 171–178.
- 399
- 400 Sanchez, C., K. D. Williams, and M. Collins, 2016: Improved stochastic physics schemes for
- 401 global weather and climate models. *Quarterly Journal of the Royal Meteorological Society*,
- 402 **142 (694)**, 147–159.
- 403
- 404 Shutts, G., M. Leutbecher, A. Weisheimer, T. Stockdale, L. Isaksen, and M. Bonavita, 2011:
- 405 Representing model uncertainty: Stochastic parametrizations at ecmwf. *ECMWF Newsletter*,
- 406 **129**, 19–24.
- 407
- 408 Thornes, T., P. D. Düben, and T. N. Palmer, 2017: On the use of scale-dependent precision in earth
- 409 system modelling. *Quarterly Journal of the Royal Meteorological Society*, **143 (703)**, 897–908.

- 406 Thornes, T., P. D. Düben, and T. N. Palmer, 2018: Scale-selective precision in the surface quasi-
- 407 geostrophic eqations.
- 408 Váňa, F., P. D. Düben, S. Lang, T. N. Palmer, M. Leutbecher, D. Salmon, and G. Carver, 2017:
- 409 Single precision in weather forecasting models: An evaluation with the ifs. *Monthly Weather*
- 410 *Review*, **145** (2), 495–502.
- 411 Weisheimer, A., S. Corti, T. Palmer, and F. Vitart, 2014: Addressing model error through atmo-
- 412 spheric stochastic physical parametrizations: impact on the coupled ecmwf seasonal forecasting
- 413 system. *Phil. Trans. R. Soc. A*, **372** (2018), 20130 290.
- 414 Wilks, D., 2006: On “field significance” and the false discovery rate. *Journal of applied meteorol-*
- 415 *ogy and climatology*, **45** (9), 1181–1189.

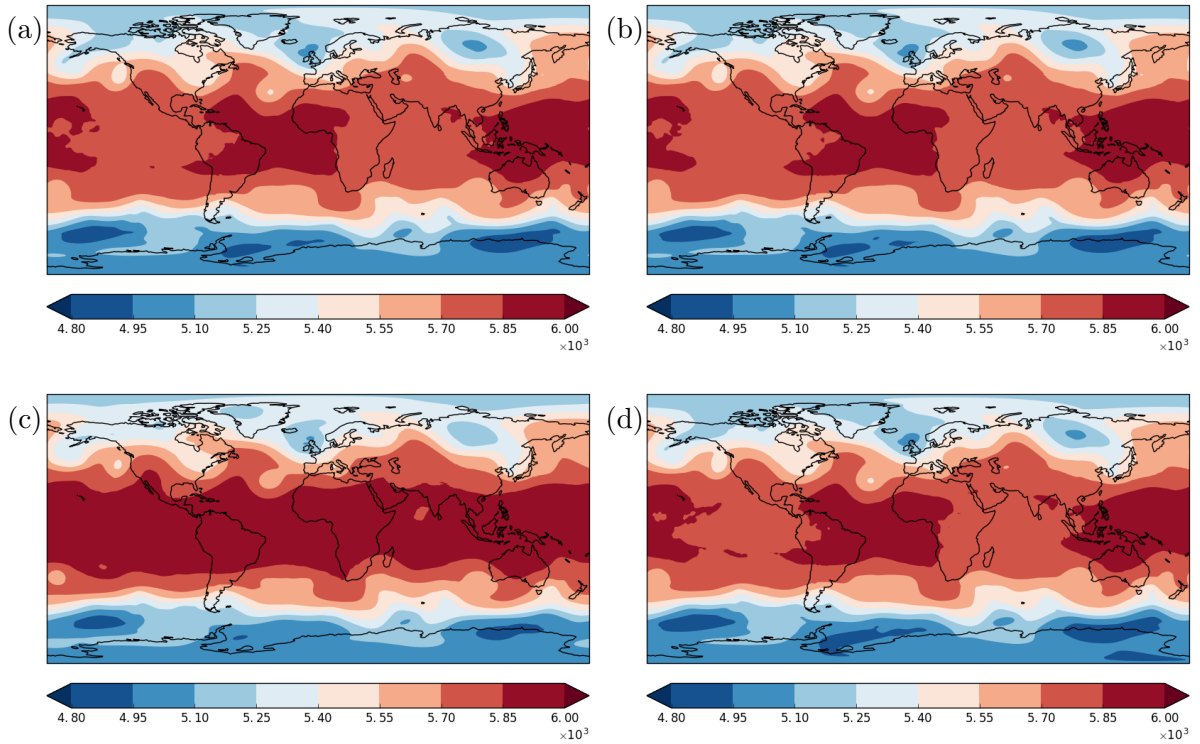
## 416 LIST OF FIGURES

417	<b>Fig. 1.</b> Evolution of hurricane Sandy at 80km resolution using OpenIFS. 3-hourly vorticity maxima 418 at pressure level 925hPa are plotted in red for simulations using 4 different precision levels 419 in spectral space. From left to right, double-precision, single-precision, 16-bit significand 420 and 8-bit significand. Although the precise position of the vorticity maxima varies between 421 all four evolutions, the hurricane landfall position and hour is reproduced even for heavy 422 precision truncations. . . . .	24
423	<b>Fig. 2.</b> Geopotential height of pressure level 500hPa after 120 simulated hours. Differences between 424 (a) double and (b) single are small, whereas at 8 significant bit (c) variations can be seen 425 globally, dominated by a global bias. (d) By retaining double-precision for the zeroth total 426 wavenumber (which includes the global mean quantities) this error is largely removed. . . . .	25
427	<b>Fig. 3.</b> (a) Precision needed to represent total wavenumbers $\geq n$ for an $L_2$ -norm error less than two. 428 Crosses represent four start-dates at T255 resolution, with the line denoting the average. (b) 429 Average precision for European ensemble error or $L_2$ error measures at resolutions T159 430 and T255. (c) Replotted T255 data as relative error against lengthscale. Please note that the 431 y-axis is reversed. (d) Total wavenumber is normalized by the truncation wavenumber to 432 collapse the data for each measure. Grey dotted lines indicate scale-selective precision used 433 for the decadal runs (see section d). . . . .	26
434	<b>Fig. 4.</b> Significance testing of decadal reduced-precision ensembles testing for differences to a 435 double-precision ensemble for the accumulated precipitation, mean 2-meter temperature 436 and mean surface pressure fields. Plotted are the local significance probabilities for single- 437 precision, weather-optimal scale-selective precision and half-precision (zeroth mode kept at 438 double-precision). Red dots indicate failed significance tests at the 5% level as calculated in 439 figure 5 . . . . .	27
440	<b>Fig. 5.</b> Top row: The local significance values from figure 4, ordered by size, to enable a global 441 assessment of significance based upon the distribution of $p$ -values. The False Discovery 442 Rate (FDR) test assesses a field as significantly different when values lie below the dashed- 443 black curve (here denoting a test at the 5% level). All local tests with $p$ -values smaller 444 than the largest failed test are considered significant and their locations are shown with red 445 dots in the spatial significance maps of figure 4. For single-precision and half-precision no 446 fields are significantly different from double-precision. The weather-optimal precision has 447 a significantly different mean surface pressure. Bottom row: The same test for ensembles 448 with the Stochastically Perturbed Parametrization Tendency (SPPT) scheme active. With 449 SPPT no fields are significant at any of the tested precisions. Here scale-selective precision 450 lies the furthest from being significant. . . . .	28
451	<b>Fig. 6.</b> Reduced precision T511 experiments compared to the distance between double- and single- 452 precision, averaged over 9 start dates after 1,2,5 and 10 days of integration. (a) Temperature 453 error for uniform precision reduction in spectral space. (b) Surface pressure error for uni- 454 form precision reduction. (c-d) Fixing global precision at 12 significand bits and using 10 455 significand bits from varying total wavenumber (indicated on the x-axis) for the same error 456 measures of temperature and surface pressure. For temperature errors beyond 1 day, 10 sig- 457 nificant bits has no increase on error for wavenumbers 7 and above. For surface pressure, 458 global 12 significand bits introduces some difference at early times which are no longer 459 significant at 5 days. . . . .	29
460	<b>Fig. 7.</b> Proportion of globe which lies more than one ECMWF ensemble standard deviation from 461 the ECMWF ensemble mean for (a) Z500 and (b) 850hPa meridional winds. Members of the	

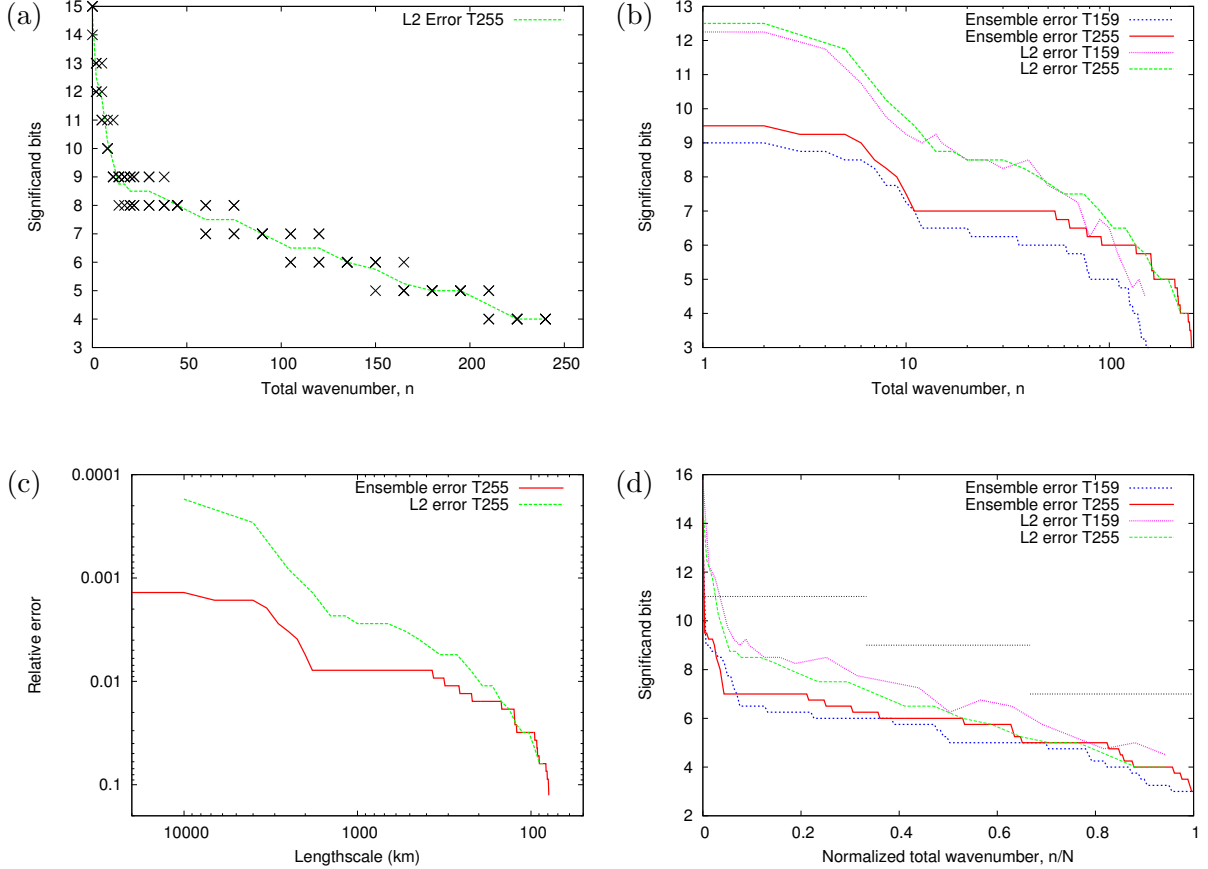
462 ECMWF ensemble remain close to a third, while the unperturbed ECMWF control climbs  
463 from zero. Our double-precision, single-precision, scale-selective and global 10 significand  
464 bits runs lie between these two, with precision choices having little influence until global  
465 precision is reduced to 9 significand bits. Model version and resolution changes are respon-  
466 sible for the difference between the ECMWF control and double-precision. . . . . 30



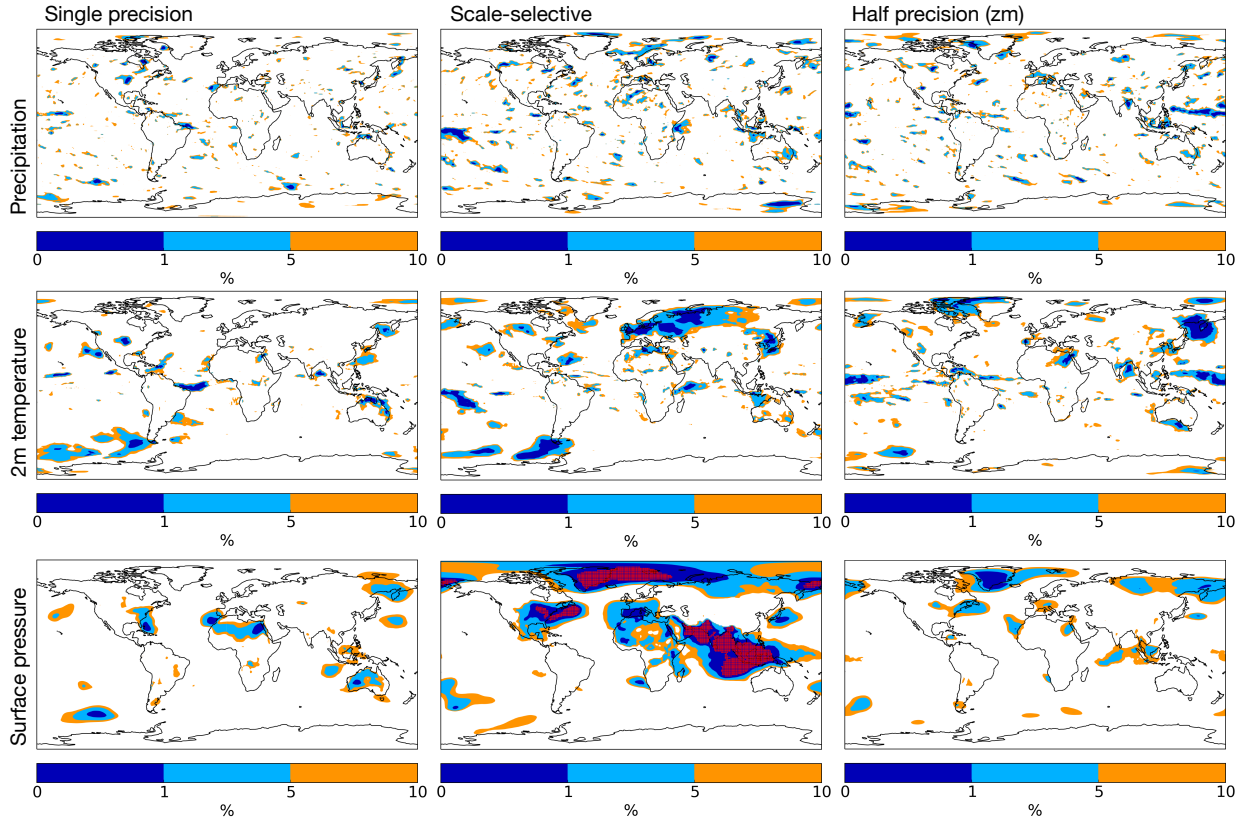
467 FIG. 1. Evolution of hurricane Sandy at 80km resolution using OpenIFS. 3-hourly vorticity maxima at pres-  
 468 sure level 925hP are plotted in red for simulations using 4 different precision levels in spectral space. From  
 469 left to right, double-precision, single-precision, 16-bit significand and 8-bit significand. Although the precise  
 470 position of the vorticity maxima varies between all four evolutions, the hurricane landfall position and hour is  
 471 reproduced even for heavy precision truncations.



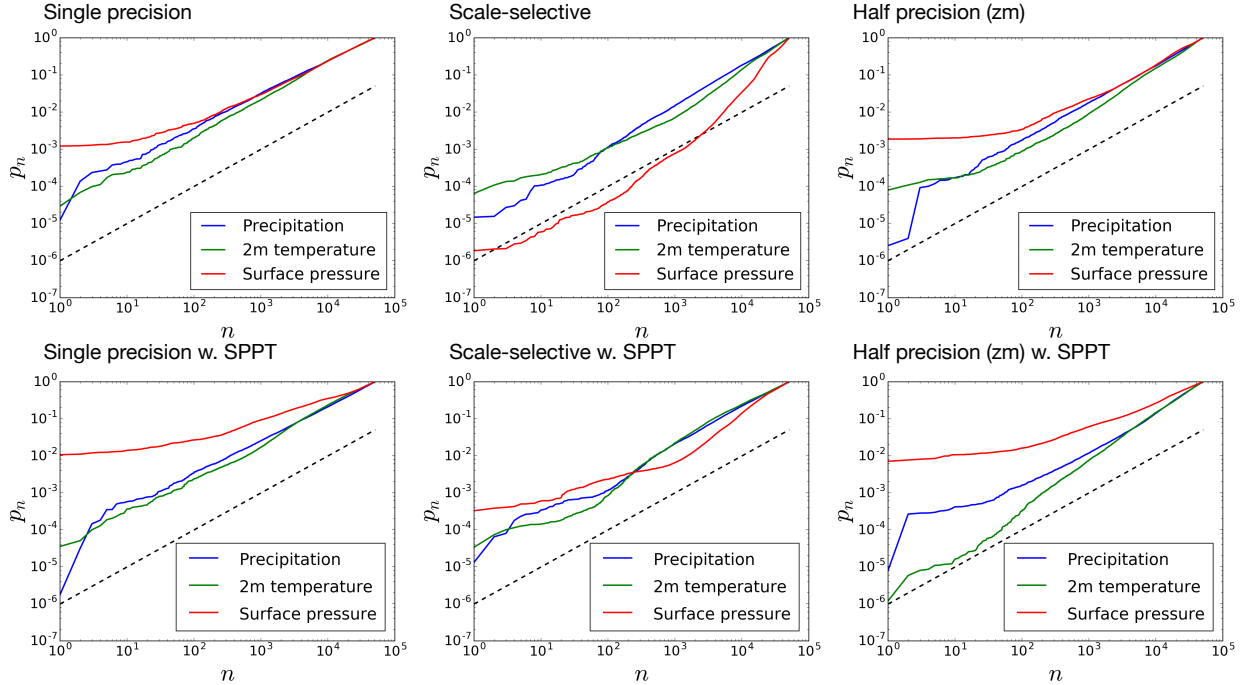
472 FIG. 2. Geopotential height of pressure level 500hPa after 120 simulated hours. Differences between (a)  
 473 double and (b) single are small, whereas at 8 significant bit (c) variations can be seen globally, dominated by a  
 474 global bias. (d) By retaining double-precision for the zeroth total wavenumber (which includes the global mean  
 475 quantities) this error is largely removed.



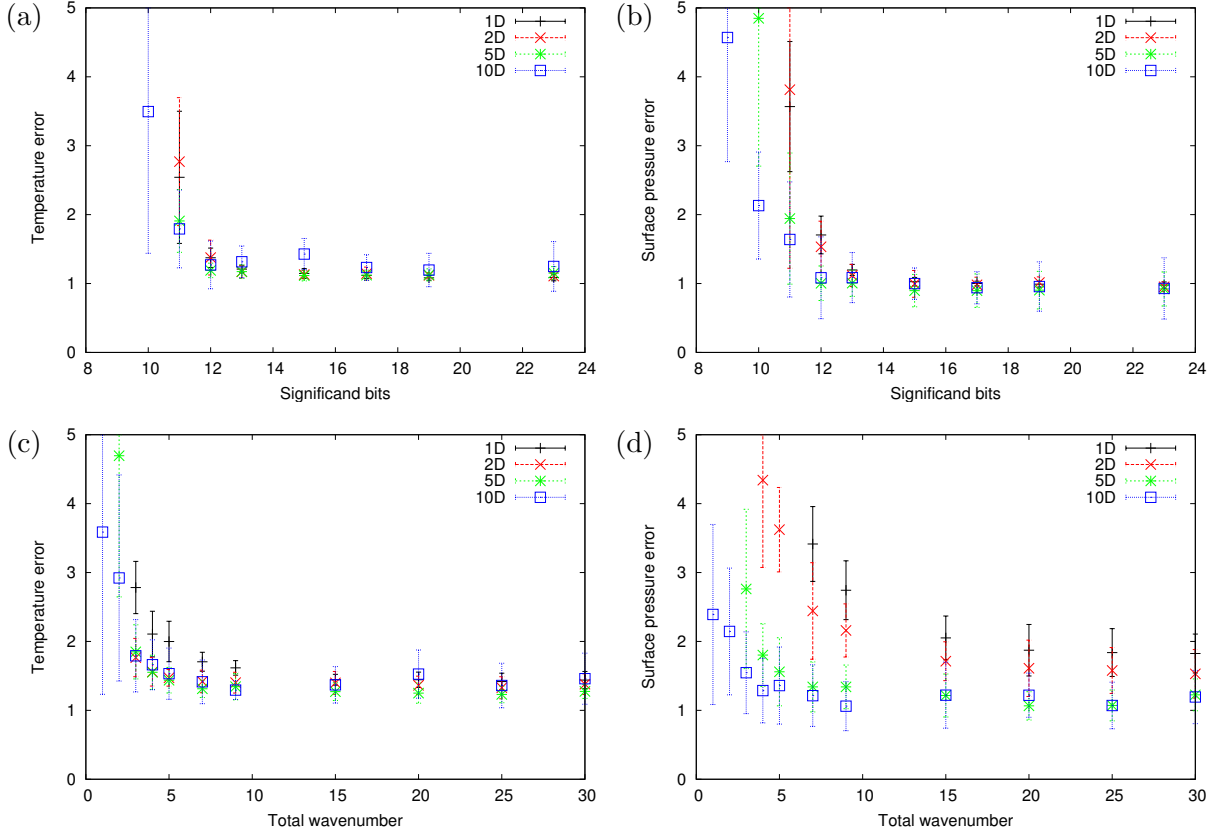
476 FIG. 3. (a) Precision needed to represent total wavenumbers  $\geq n$  for an  $L_2$ -norm error less than two. Crosses  
 477 represent four start-dates at T255 resolution, with the line denoting the average. (b) Average precision for  
 478 European ensemble error or  $L_2$  error measures at resolutions T159 and T255. (c) Replotted T255 data as relative  
 479 error against lengthscale. Please note that the y-axis is reversed. (d) Total wavenumber is normalized by the  
 480 truncation wavenumber to collapse the data for each measure. Grey dotted lines indicate scale-selective precision  
 481 used for the decadal runs (see section d).



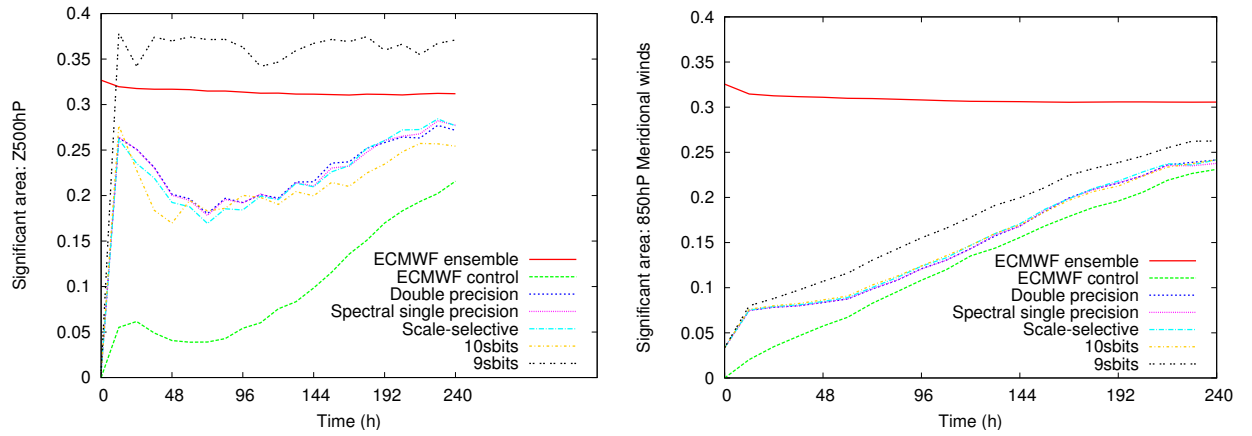
482 FIG. 4. Significance testing of decadal reduced-precision ensembles testing for differences to a double-  
 483 precision ensemble for the accumulated precipitation, mean 2-meter temperature and mean surface pressure  
 484 fields. Plotted are the local significance probabilities for single-precision, weather-optimal scale-selective pre-  
 485 cision and half-precision (zeroth mode kept at double-precision). Red dots indicate failed significance tests at the  
 486 5% level as calculated in figure 5



487 FIG. 5. Top row: The local significance values from figure 4, ordered by size, to enable a global assessment of  
 488 significance based upon the distribution of  $p$ -values. The False Discovery Rate (FDR) test assesses a field as sig-  
 489 nificantly different when values lie below the dashed-black curve (here denoting a test at the 5% level). All local  
 490 tests with  $p$ -values smaller than the largest failed test are considered significant and their locations are shown  
 491 with red dots in the spatial significance maps of figure 4. For single-precision and half-precision no fields are  
 492 significantly different from double-precision. The weather-optimal precision has a significantly different mean  
 493 surface pressure. Bottom row: The same test for ensembles with the Stochastically Perturbed Parametrization  
 494 Tendency (SPPT) scheme active. With SPPT no fields are significant at any of the tested precisions. Here  
 495 scale-selective precision lies the furthest from being significant.



496 FIG. 6. Reduced precision T511 experiments compared to the distance between double- and single-precision,  
497 averaged over 9 start dates after 1,2,5 and 10 days of integration. (a) Temperature error for uniform precision  
498 reduction in spectral space. (b) Surface pressure error for uniform precision reduction. (c-d) Fixing global  
499 precision at 12 significand bits and using 10 significand bits from varying total wavenumber (indicated on the  
500  $x$ -axis) for the same error measures of temperature and surface pressure. For temperature errors beyond 1 day,  
501 10 significand bits has no increase on error for wavenumbers 7 and above. For surface pressure, global 12  
502 significand bits introduces some difference at early times which are no longer significant at 5 days.



503 FIG. 7. Proportion of globe which lies more than one ECMWF ensemble standard deviation from the ECMWF  
 504 ensemble mean for (a) Z500 and (b) 850hP meridional winds. Members of the ECMWF ensemble remain close  
 505 to a third, while the unperturbed ECMWF control climbs from zero. Our double-precision, single-precision,  
 506 scale-selective and global 10 significand bits runs lie between these two, with precision choices having little  
 507 influence until global precision is reduced to 9 significand bits. Model version and resolution changes are  
 508 responsible for the difference between the ECMWF control and double-precision.